

Monitoring of Plant Chlorophyll and Nitrogen Status Using the Airborne Imaging Spectrometer AVIS

Dissertation
der Fakultät für Geowissenschaften
der Ludwig-Maximilians-Universität München

Vorgelegt von:
Natascha Oppelt

Eingereicht: April 2002

1. Gutachter: Prof. Dr. W. Mauser

2. Gutachter: Prof. Dr. F. Wieneke

Tag der mündlichen Prüfung: 12.07.2002

„Don't panic“
(Douglas Adams)

Table of Contents

Table of Contents.....	I
List of Figures.....	V
List of Tables.....	XI
List of Abbreviations.....	XIV
Acknowledgements.....	XVI
1 Introduction.....	1
1.1 Hyperspectral Remote Sensing and Imaging Spectrometry	5
1.2 Importance of Chlorophyll and Nitrogen	8
2 AVIS – the Airborne Visible/Near Infrared Imaging Spectrometer.....	10
2.1 System Description.....	10
2.1.1 Camera Unit	11
2.1.1.1 Spectrograph	12
2.1.1.2 Camera	13
2.1.1.3 Lens.....	16
2.1.1.4 Filter... ..	16
2.1.2 Storage Unit	18
2.1.2.1 Personal Computer	18
2.1.2.2 Differential GPS (dGPS)	18
2.2 Radiometric Properties.....	19
2.2.1 Dark Current.....	19
2.2.2 Homogeneity of the CCD Array.....	21
2.3 Spectral Properties	23
2.3.1 Spectral Resolution.....	23
2.3.2 Spectral Sampling Interval	24
2.3.3 Centre Wavelengths	24
2.4 Signal to Noise Ratio (SNR).....	27
2.5 Geometric Properties	31
2.5.1 Spatial Resolution.....	31
2.5.2 Field of View and Instantaneous Field of View	32
2.6 Summary.....	34
3 Test Sites and Ground Measurements (Ground Truth).....	36
3.1 Test Area Starnberg	37
3.1.1 Test Site Gilching	40
3.1.2 Test Site Inning	42

3.1.3	Test Site Frieding	44
3.2	Investigated Land Cover Types	46
3.2.1	Wheat (<i>Triticum aestivum L.</i>)	46
3.2.2	Maize (<i>Zea mays L.</i>)	47
3.2.3	Grassland	47
3.3	Ground Measurements.....	52
3.3.1	The Ground Measurements	54
3.3.1.1	Weekly Measured Plant Parameters	55
3.3.1.1.1	Phenological Status	55
3.3.1.1.2	Plant Height of Crops.....	56
3.3.1.1.3	Plant Height of Grassland.....	56
3.3.1.1.4	Photographs	57
3.3.1.1.5	Wet Biomass.....	57
3.3.1.1.6	Dry Biomass	57
3.3.1.2	Additional Ground Measurements	58
3.3.1.2.1	Land Cover Mapping.....	58
3.3.1.2.2	Floristic Mapping of Grassland	58
3.3.1.2.3	Management Data.....	59
3.3.1.2.4	Yield Measurement.....	60
3.3.1.3	Derived Plant Parameters.....	60
3.3.1.3.1	Plant Chlorophyll Content.....	60
3.3.1.3.2	Plant Nitrogen Content	62
3.4	Investigated Plants.....	63
3.4.1	Wheat (<i>Triticum aestivum L.</i>)	63
3.4.2	Maize (<i>Zea mays L.</i>)	67
3.4.3	Grassland	72
3.4.3.1	Meadow with one cut	73
3.4.3.2	Meadow with two cuts.....	75
3.4.3.3	Meadow with rotational grazing.....	77
3.4.3.4	Meadow with four to five cuts	79
3.4.4	Field Spectrometer Data	83
3.4.4.1	DLR Reference Target	83
3.4.4.2	Ground Measurements of Test Fields	84
4	Airborne Measurements and Preprocessing of the Data.....	86
4.1	The flight campaigns 1999 and 2000	87
4.2	Data Preprocessing	89
4.2.1	Dark Current and Flat Field Correction	89
4.2.2	Resampling to 80 Bands	89
4.2.3	Atmospheric Correction and Reflectance Calibration	91

4.2.3.1	Calibration into Radiances.....	93
4.2.3.2	Definition of Atmospheric Conditions.....	94
4.2.3.3	Atmospheric Modelling with LOWTRAN-7.....	95
4.2.3.4	Consideration of the Sensor Characteristics	95
4.2.3.5	Reflectance Calibration	96
4.2.4	Validation of the Preprocessed Data.....	96
4.2.4.1	1999... ..	97
4.2.4.2	2000... ..	98
4.2.5	Directional effects	99
4.2.6	Results of the Preprocessing	101
4.2.6.1	Wheat.....	103
4.2.6.2	Maize.. ..	104
4.2.6.3	Grassland	105
4.3	Geometric Rectification	108
5	Derivation of Plant Chlorophyll and Nitrogen Status with Hyperspectral Remote Sensing.....	112
5.1	Chlorophylls.....	114
5.2	Measured Nitrogen – Chlorophyll Correlation	117
5.2.1	Wheat.....	117
5.2.2	Maize	121
5.2.3	Grassland	124
5.2.4	Conclusions	126
5.3	Spectral Properties of Plant Leaves	128
5.4	Spectral Properties of Plant Canopies.....	130
5.4.1	Biophysical Attributes of a Canopy	130
5.4.1.1	Canopy Density (Leaf area Index).....	130
5.4.1.2	Soil Background	131
5.4.1.3	Leaf Orientation	132
5.4.1.4	Viewing Geometry	132
5.5	Approaches for the Derivation of Chlorophyll and Nitrogen Content of Plants.....	135
5.5.1	The Normalised Difference Vegetation Index (NDVI)	135
5.5.2	Optimised Soil-Adjusted Vegetation Index (OSAVI)	137
5.5.3	Chlorophyll Absorption Integral (CAI).....	137
5.5.4	Results of the Chlorophyll and Nitrogen Derivation.....	138
5.5.4.1	Wheat.....	139
5.5.4.2	Maize.. ..	143
5.5.4.3	Grassland	147
5.5.5	Discussion of the Results	149

6	Spatial Distribution of Chlorophyll and Nitrogen Content within a Wheat Canopy.....	154
6.1	Ground Truth and AVIS Measurements	154
6.2	Hyperspectral Approaches Used for the Derivation of Chlorophyll and Nitrogen within the Field.....	157
6.2.1	Chlorophyll a Content per Area.....	157
6.2.2	Chlorophyll a Content per Mass	158
6.2.3	Nitrogen Content per Area	159
6.2.4	Nitrogen Content per Mass.....	160
6.3	Spatial Patterns of Nitrogen within the Field	162
7	Summary and Outlook.....	165
8	Zusammenfassung.....	170
9	References.....	176
	Appendix.....	189
	Appendix 1: AVIS Centre Wavelengths for the 2nm Resampling	189
	Appendix 2: Results of the Botanical Mapping of Grassland.....	191
	Appendix 3: Code for "Day Of Year" (DOY) Dates	192
	Appendix 4: Regression Equations of the Spectral Approaches which have the Strongest Significant Relationship with the Chlorophyll and Nitrogen Content for Wheat and Maize.....	193

List of Figures

Figure 1-1:	Structure of the thesis	3
Figure 1-2:	Electromagnetic spectrum (Kappas, 1994, modified; cartography: V. Falck).....	5
Figure 1-3:	Dispersion of light by a prism.....	6
Figure 1-4:	Hyperspectral image cube (based on NASA diagram; cartography: V.Falck). 7	
Figure 2-1:	AVIS schematic (Oppelt & Mauser, 2000)	10
Figure 2-2:	AVIS mounted into the aircraft.....	11
Figure 2-3:	AVIS camera unit with CCD camera, spectrograph, lens and filter (SPECTRAL IMAGING LTD., 1998a)	11
Figure 2-4:	Schematic diagram of spectrograph ImSpector (SPECTRAL IMAGING LTD., 1998a).....	12
Figure 2-5:	Diffraction efficiency of spectrograph grating (SPECTRAL IMAGING LTD., 1998c).....	13
Figure 2.6:	Spectral responsivity of camera C5999 (HAMAMATSU, 1998).....	15
Figure 2-7:	Spectral responsivity of lens SCHNEIDER CNG 1.4/8 (SCHNEIDER, 1998) ...	16
Figure 2-8:	Spectral responsivity product of lens, spectrograph and camera (blue) and transmission curve of filter SCHOTT BG 26 (SCHOTT, 1999)	17
Figure 2-9:	Spectral responsivity of AVIS	17
Figure 2-10:	Dark Current matrix measured for 1999 (left) and 2000 (right) at a sensor temperature of 15°C.....	20
Figure 2-11:	Dependency of dark current on sensor temperature measured for 1999 (left) and 2000 (right).....	20
Figure 2-12:	Gain matrices for 1999 (left) and 2000 (right).....	22
Figure 2-13:	Spectral resolution, spectral sampling interval, FWHM and centre wavelength of a Gaussian response function (Schaepman, 1998).....	23
Figure 2-14:	LOWTRAN simulation of radiances of skylight for 0.5 and 6nm spectral resolution compared with AVIS spectrum (Oppelt & Mauser, 2000).....	24
Figure 2-15:	Wavelength calibration of AVIS using an Argon emission lamp; the table presents the wavelengths of the reflection peaks in nm; NBoS = National Bureau of Standards (Oppelt & Mauser, 2000)	25
Figure 2-16:	AVIS SNR analysis 1999 for a spectral sampling interval of 2nm (left) and 6nm (right); sigma is the standard deviation; illumination source: Tungsten halogen lamp (Oppelt & Mauser, 2000)	28
Figure 2-17:	AVIS SNR analysis 2000 for a spectral sampling interval of 6nm; sigma is the standard deviation; illumination source: Tungsten halogen lamp.....	29
Figure 2-18:	AVIS SNR analysis 2000 for spectral sampling interval of 6nm; sigma is the standard deviation; illumination source: sunlight.....	30
Figure 2-19:	Illustration of a brightness ramp (Oppelt & Mauser, 2000)	31

Figure 2-20: Spectral responsivity of AVIS.....	35
Figure 3-1: Location of the natural units of the test area Starnberg (cartography: V. Falck).....	38
Figure 3-2: Monthly precipitation measured at the weather stations Hüll (left) and Rothenfeld (right) during 1999 and 2000.....	39
Figure 3-3: Soil texture (left) (source: Geologisches Landesamt, 1980) and elevation (right) in the test site Gilching (data source: Bayerisches Landesvermessungsamt, 1999).....	41
Figure 3-4: Land cover maps for 1999 (left) and 2000 (right)	42
Figure 3-5: Map of soil texture (left) (data source: Geologisches Landesamt, 1986) and digital elevation (right) of the test site Inning (data source: MILGEO) ..	43
Figure 3-6: Land cover in the test site Inning for 1999 (left) and 2000 (right)	44
Figure 3-7: Digital elevation map (left) (Data source: MILGEO) and land cover Mapping (right) for the test site Frieding 1999.....	45
Figure 3-8: Structure of a grassland canopy (Riegler et al., 1998; modified).....	49
Figure 3-9: Effect of the type of cultivation on the biological diversity of grassland (Ellenberg, 1996; modified)	50
Figure 3-10: Connection between nutrient supply and occurrence of species in a fresh (oatgrass) meadow (<i>Arrhenatherion elatioris</i>) (Spatz, 1994)	51
Figure 3-11: Positions of the test fields for 1999 and 2000 as well as locations of the weather stations (cartography: V.Falck)	53
Figure 3-12: Location of the sampling points within a test field of wheat	54
Figure 3-13: Measurement report for wheat.....	55
Figure 3-14: Photographs of wheat; side view (left), overview (centre) and top view (right).....	57
Figure 3-15: Data sheet of the "Schlagkartei" for a field of winter wheat	59
Figure 3-16: Chlorophyll absorption spectra of sun leaves of grassland at two different sampling dates	61
Figure 3-17: Photographs of field No.93 for the year 1999: left=during stem elongation (EC 37) (DAS 200=10 th May); centre=end of emergence of the inflorescence (EC 59) (DAS 228=7 th June); right=beginning of ripening (EC 91) (DAS 284=2 nd August).....	64
Figure 3-18: Development of plant height, dry biomass, nitrogen and chlorophyll content for wheat during the growing period 1999 as measured on field No.93.....	66
Figure 3-19: Photographs of field No.260 for the year 1999: left=during tillering (EC 25) (DAS 65=5 th July); centre=begin of milk development (EC 73) (DAS 93= 2 nd August); right=dough development (EC 82) (DAS 128=6 th September) ..	68
Figure 3-20: Development of plant height, dry biomass, nitrogen and chlorophyll content for maize during the growing period 1999 as measured on field No.260	70

Figure 3-21: Dependence of chlorophyll a content per mass of the daily mean temperature derived from field measurements of maize field No.52 and weather station Hüll (the dotted blue line represents 15°C)	71
Figure 3-22: Photographs of meadow No.106a for the year 1999: left=first growth on DOY 123 (3 rd May); centre=first regrowth on DOY 200 (19 th July); right=first regrowth on DOY 263 (20 th September)	73
Figure 3-23: Development of plant height, dry biomass, nitrogen and chlorophyll content for the extensively used meadow No.106a during the growing period 1999.	74
Figure 3-24: Development of plant height, dry biomass, nitrogen and chlorophyll content for the extensive meadow No.224 during the growing period 1999	76
Figure 3-25: Photographs of the test meadow No.224 for the year 1999: left=first growth at DOY 123 (3 rd May); centre=first regrowth at DOY 200 (19 th July); right=second regrowth at DOY 263 (20 th September)	77
Figure 3-26: Photographs of the test meadow No.53b for the year 1999: far left=first growth at DOY 123 (3 rd May); centre left=first regrowth at DOY 172 (21 st June); centre right=second regrowth after grazing at DOY 208 (26 th July); far right=third regrowth at DOY 242 (30 th August).....	78
Figure 3-27 Development of plant height, dry biomass, nitrogen and chlorophyll content for the intensive meadow No.53b during the growing period 1999	79
Figure 3-28: Photographs of the test meadow No.224 for the year 1999: far left=first growth at DOY 116 (26 th April); centre left=first regrowth at DOY 158 (7 th July); centre right=second regrowth at DOY 207 (26 th July); far right=third regrowth at DOY 263 (20 th September).....	80
Figure 3-29: Development of plant height, dry biomass, nitrogen and chlorophyll content for the intensive meadow No.223 during the growing period 1999	81
Figure 3-30: Position of the DLR reference field (left) and a reflectance spectrum measured in 1999	84
Figure 3-31: SIRIS reflectance spectra of different land covers measured on 3 rd July 1999.....	84
Figure 4-1: Campaigns calendars for 1999 and 2000 (green triangles=ground measurements; red triangles= AVIS measurements).....	87
Figure 4-2: Flight stripes within the test area on 18 th July 1999, flown at 4000ft (blue) and 10000ft asl (green); the red numbers represent the position of the test fields	88
Figure 4-3: AVIS preprocessing steps.....	89
Figure 4-4: Effects of averaging for an AVIS grey value spectrum (Oppelt & Mauser, 2000).....	90
Figure 4-5: Deviation of the oxygen absorption position from the nominal band No.103.7 (=761nm; left) and corrected wavelength shift after the oxygen alignment (right).....	91

Figure 4-6: Atmospheric transmittance and main absorbers in the VIS and NIR spectral region, modelled with a spectral resolution of 6nm using LOWTRAN-7.....	92
Figure 4-7: Sequence of PULREF processing steps (Bach, 1995; modified).....	93
Figure 4-8: Modelled spectral radiances and measured grey values of the DLR hangar for the 18 th July 1999 (left) and gain values for 1999 and 2000 (right) for a spectral resolution of 6nm	94
Figure 4-9: Modelled ground (left) and path (right) radiance using LOWTRAN-7 for the 18 th July 1999 with a spectral resolution of 6nm.....	95
Figure 4-10: Modelled total at-sensor radiance using LOWTRAN-7 for the 18 th July 2000 with a spectral resolution of 6nm	96
Figure 4-11: AVIS reflectance spectra for 1999 for individual pixels (left) and field average (right), measured at field No. 52 on 18 th July 1999; altitude: 4000ft asl.....	97
Figure 4-12: AVIS reflectance spectra for 2000 for individual pixels (left) and mean field spectrum (right), measured at field No. 146a on 22 nd July 2000; altitude: 4000ft asl.....	98
Figure 4-13: Field average spectra of maize field No.260 at 4000 and 1000ft asl, flown on 19 th July 1999 (upper graph) and differences between the two spectra (lower graph).....	100
Figure 4-14: Mean highway spectra from 9 th May 1999 (left; position of the pixel in Z= row; S=column) and comparison of different acquisition dates (right)	101
Figure 4-15: AVIS raw data image (left) and processed image (right) (R/G/B = 582/674/729nm) with associated grey value and reflectance spectra of different land cover types, acquired on 19 th July 1999.....	102
Figure 4-16: Development of a wheat canopy (field No.93) throughout the vegetation period 1999.....	104
Figure 4-17: Development of a maize canopy (field No.65a) throughout the vegetation period 1999.....	104
Figure 4-18: Development of a meadow with one cut (No. 106a) during the vegetation period 1999.....	107
Figure 4-19: Image distortions due to altitude (a), velocity (b), pitch (c), roll (d) and yaw (e) (Richards, 1998).....	109
Figure 4-20: Geometric correction of preprocessed AVIS data (left) with dGPS data (geographical position, flight altitude as well as velocity of the aircraft) and resulting geometrically corrected image (right) (R/G/B = 582/674/729nm), acquired on 19 th July 1999.....	110
Figure 4-21: Mosaic of the test site Gilching assembled using flight strips acquired on 3 rd and 10 th May 2000	111
Figure 5-1: Scattering processes of light in a leaf (Guyot et al., 1992).....	112
Figure 5-2: Chemical structure of chlorophyll (Hopkins, 1995)	114

Figure 5-3: In vivo (continuous line) and in vitro (dotted line) chlorophyll absorption of an vital plant leaf (Schellberg, 1990)	115
Figure 5-4: Relation of chlorophyll a (left) and b (right) content per area to nitrogen content per area for wheat measured during the ground measurements 1999 and 2000.....	118
Figure 5-5: Schematic representation of the development of nitrogen and chlorophyll content during a vegetation period for wheat canopies derived from field measurements in 1999 and 2000 (the second number in the table is the standard deviation from the mean content values).....	119
Figure 5-6: Relation of chlorophyll a (left) and b (right) content per area to nitrogen content per area for maize canopies derived from field measurements in 1999 and 2000.....	121
Figure 5-7: Schematic representation of the development of the nitrogen and chlorophyll content during a vegetation period for maize derived from field measurements in 1999 and 2000 (the second number in the table is the standard deviation of the mean content values).....	123
Figure 5-8: Correlation of chlorophyll a (left) and b (right) content per area to nitrogen content per area for grassland canopies derived from field measurements in 1999 and 2000.....	124
Figure 5-9: Schematic presentation of the development of nitrogen and chlorophyll content during a vegetation period for grassland derived from field measurements in 1999 and 2000 (the second number in the table is the standard deviation of the mean content values).....	125
Figure 5-10: Parameters influencing the spectral reflectance of green vegetation (Bach, 1995; modified)	128
Figure 5-11: Dependency of the spectral reflectance of a lime leaf on water content (Bach, 1995; modified)	129
Figure 5-12: Spectral reflectance of an oak leaf during growth and senescence (Gates et al., 1965)	129
Figure 5-13: Difference in reflectance due to LAI variations (Asner, 1998)	131
Figure 5-14: Dependency of the reflectance of a sandy to silty soil on the soil moisture (left) and soil type (right) (Bach, 1995; modified)	131
Figure 5-15: Effect of changing mean leaf angle (MLA) on canopy reflectance, simulated with a LAI=5.0 (Asner, 1998).....	132
Figure 5-16: Basic forms of scattering distribution: diffuse scattering (left), forward scattering (centre); backward scattering (right) (Gerstl, 1988)	133
Figure 5-17: BRDF of an aspen forest in the red (670nm; left) and NIR (870nm; right) for a sun zenith angle of 50°, ρ_λ = reflectance (ESA, 1999)	133
Figure 5-18: Principle of CAI measurement (left) and changes in chlorophyll absorption due to plant senescence (URL2)	138

Figure 5-19: Plot of linear correlations between indices and chlorophyll/nitrogen content for wheat derived from field and AVIS measurements in 1999 and 2000 ..	140
Figure 5-20: Linear correlations between indices and chlorophyll/nitrogen content for maize derived from field and AVIS measurements in 1999 and 2000.....	144
Figure 5-21: Linear correlations between indices and chlorophyll/nitrogen content for grassland derived from field and AVIS measurements in 1999 and 2000 ..	148
Figure 6-1: Photograph of the test field No.400 taken during the AVIS overflight on 2 nd June 2000.....	154
Figure 6-2: Development of the chlorophyll and nitrogen content within field No.400, cultivar Bussard, derived from field measurements in the year 2000	155
Figure 6-3: Campaign calendar for the wheat fields No.400 (Bussard) in the year 2000.....	156
Figure 6-4: Measured and calculated chlorophyll a content per area with rmse for field No.400 in the year 2000 (rmse=root mean square error).....	158
Figure 6-5: Measured and calculated chlorophyll a content per mass with rmse for field No.400 in the year 2000.....	159
Figure 6-6: Measured and calculated nitrogen content per area with rmse for field No.400 in the year 2000.....	160
Figure 6-7: Measured and calculated nitrogen content per mass with rmse for field No.400 in the year 2000.....	161
Figure 6-8: CAI images derived from AVIS measurements in 2000 and yield measurement map of wheat field No.400.....	163

List of Tables

Table 2-1:	Parameters of spectrograph ImSpector V9-M-897 (SPECTRAL IMAGING LTD., 1998b).....	13
Table 2-2:	Camera C5999 (HAMAMATSU) specifications (HAMAMATSU, 1998)	14
Table 2-3:	Parameters of lens SCHNEIDER CNG 1.4/8 (SCHNEIDER, 1998)	16
Table 2-4:	Centre wavelengths for the averaged band AVIS setuo with a spectral resolution of 6nm	26
Table 2-5:	AVIS SNR.....	30
Table 2-6:	Pixel size, spatial resolution and FOV at different flight altitudes with resulting frame rates.....	33
Table 2-7:	AVIS parameters	34
Table 3-1:	Location of the test area Starnberg	37
Table 3-2:	Mean average precipitation and average temperature within the test area (time period 1931 – 1960) measured at the weather stations Hüll and Rothenfeld (1999 and 2000) (Demircan 1995; Grottenthaler, 1980; Stolz, 1998; data of the "Agrarmet. Messnetz Bayern" 1999 and 2000)	40
Table 3-3:	Distribution of land cover types within the test site Gilching 1999 and 2000	42
Table 3-4:	Distribution of land cover types within the test site Inning 1999 and 2000..	43
Table 3-5:	Distribution of land cover types within the test site Frieding 1999	45
Table 3-6:	Requirements of winter wheat regarding climate, soil and water supply (Franke, 1989; Stolz, 1998)	46
Table 3-7:	Requirements of maize regarding climate, soil and water supply (Franke, 1989; Heyland, 1996)	47
Table 3-8:	Requirements of grassland of the temperate zone regarding climate, soil and water supply (Heyland, 1996; Whitehead, 1995)	48
Table 3-9:	Principal growth stages of cereals (Zadoks et al., 1974)	56
Table 3-10:	Test fields for winter wheat and availability of additional data (acronyms: S = Schlagkartei; Y = yield estimation; - = no data available)	63
Table 3-11:	Test fields for maize and availability of additional data (acronyms: EC=electric conductivity; S=Schlagkartei; Y=yield estimation; - = no data available)	68
Table 3-12:	Characterisation of the grassland test fields in 1999/2000 and availability of Schlagkartei data (S) (- = no data available) (the Klapp value is weighted and normalised to maximum)	73
Table 4-1:	Differences of maize reflectances due to different altitudes for two AVIS measurement dates (sun elevation is calculated for sea level at 47°57'N 11°17'E)	100
Table 4-2:	Coverage of wheat test fields during the flight campaigns 1999 and 2000	103

Table 4-3:	Coverage of maize test fields during the flight campaigns 1999 and 2000.	105
Table 4-4:	Coverage of test meadows during the flight campaigns 1999 and 2000....	106
Table 5-1:	Comparison of significant features of C3 and C4 plants (Hopkins, 1995)...	116
Table 5-2:	Significant correlations between nitrogen and chlorophyll content of leaves for wheat canopies (r=coefficient of correlation, r ² =coefficient of determination, p=statistical significance level).....	118
Table 5-3:	Significant correlations between nitrogen and chlorophyll content of leaves for wheat canopies considering the phenological stage (before/after EC 40) (r=coefficient of correlation, r ² =coefficient of determination, p=statistical significance level, n.s.=not significant)	120
Table 5-4:	Significant correlations between nitrogen and chlorophyll content for maize leaves (r=coefficient of correlation, r ² =coefficient of determination, p=statistical significance level).....	121
Table 5-5:	Significant correlations between nitrogen and chlorophyll for maize leaves considering the cultivar (r=coefficient of correlation, r ² =coefficient of determination, p=statistical significance level, n.s.=not significant).....	122
Table 5-6:	Significant correlations between nitrogen content and chlorophyll trend per mass for the maize cultivars (r=coefficient of correlation, r ² =coefficient of determination, p=statistical significance level).....	123
Table 5-7:	Significant correlations between nitrogen and chlorophyll for grassland canopies (r=coefficient of correlation, r ² =coefficient of determination, p=statistical significance level).....	124
Table 5-8:	Significant correlations between nitrogen and chlorophyll for the grassland sites (r=coefficient of correlation, r ² =coefficient of determination, p=statistical significance level).....	125
Table 5-9:	Significantly high coefficients of determination using linear correlation equations for wheat, derived without consideration of the cultivar	139
Table 5-10:	Significantly high coefficients of determination (r ² ≥0.67) using linear correlation equations for wheat, derived for the cultivar Bussard	141
Table 5-11:	Significantly high coefficients of determination (r ² ≥0.67) using linear correlation equations for wheat, derived from the cultivar Capo.....	142
Table 5-12:	Mean parameter values and standard deviations (Std) of wheat cultivars Bussard and Capo.....	143
Table 5-13:	Significantly high coefficients of determination (r ² ≥0.67) for maize, derived without consideration of cultivars	145
Table 5-14:	Mean parameter values and standard deviations (Std) of maize cultivars Bristol/Korus, Magister and Narval	145
Table 5-15:	Significantly high coefficients of determination (r ² >0.67) for the maize cultivar Magister	147

Table 5-16: Significantly high coefficients of determination ($r^2 > 0.67$) for the maize cultivar Narval	147
Table 5-17: Significantly high coefficients of determination ($r^2 \geq 0.67$) for the meadow No.223 with four to five cuts	149
Table 5-18: Parameter values with respect to the particular saturation limit derived for the grassland sites (Std=standard deviation)	149
Table 5-19: Spectral approaches having the strongest relationship to pigment content on the basis of the coefficient of determination for wheat and maize canopies without consideration of the cultivar or phenological stage (- = no significant correlation could be derived)	150
Table 7-1: AVIS characteristics	165
Tabelle 8-1: AVIS Spezifikationen.....	171

List of Abbreviations

AIS	Airborne Imaging Spectrometer
asl	above sea level
AVIRIS	Airborne Visible/InfraRed Imaging Spectrometer
AVIS	Airborne Visible/near Infrared imaging Spectrometer
BAHC	Biological Aspects of the Hydrological Cycle
BITÖK	Bayreuther Institut für Terrestrische Ökosystemforschung (Bayreuth's institute for terrestrial ecosystem research)
BRDF	Bidirectional Reflectance Distribution Function
C	Carbon
CAI	Chlorophyll Absorption Integral
CASI	Compact Airborne Spectrographic Imager
CCD	Charge-Coupled Device
CET	Central European Time
Chl	Chlorophyll
CHRIS	Compact High Resolution Imaging Spectrometer
DAIS	Digital Airborne Imaging Spectrometer
DAS	Days After Sowing
DC	Dark Current
DFD	Deutsches Fernerkundungs-Datenzentrum (Germany's remote sensing data centre)
DFG	Deutsche Forschungsgemeinschaft (German research community)
dGPS	differential Geographical Positioning System
DLR	Deutsches Zentrum für Luft- und Raumfahrt (German aerospace centre)
DM	Dry Matter
DN	Digital Number
DOY	Day Of Year
DWD	Deutscher Wetter Dienst (German weather service)
EC	Eucarpia Code
EO-1	Earth Observation 1
FOV	Field of View
FWHM	Full Width Half Maximum
GIS	Geographical Information System
GPS	Geographical Positioning System

GSF	Forschungszentrum für Umwelt und Gesundheit (research centre for environment and health)
H	Hydrogen
hNDVI	hyperspectral NDVI
HYMAP	HYperspectral MAPping
IFOV	Instantaneous Field of View
IR	InfraRed
LAI	Leaf Area Index
Mg	Manganese
MIR	Mid InfraRed
MLA	Mean Leaf Angle
N	Nitrogen
NBoS	National Bureau of Standards
NASA	National Aeronautics and Space Administration, USA
NDVI	Normalised Difference Vegetation Index
NIR	Near InfraRed
nm	nanometer
NN	Normal Null
O	Oxygen
OSAVI	Optimised Soil Adjusted Vegetation Index
p	statistical significance level
Pixel	Picture element
Proba	Project for on-board autonomy
PULREF	Procedure to Use Lowtran for REFlectance calibration
rmse	root mean square error
ROSIS	Reflectance Optics System Imaging Spectrometer
SNR	Signal to Noise Ratio
SPECTRA	Surface Processes and Ecosystems Changes Through Response Analysis
SWIR	Short Wave InfraRed
TM	Thematic Mapper
VIS	VISible
µm	micrometer

Acknowledgements

Usually geographers are on the user's end of imaging spectrometers. Concerning oneself with the technical side of spectrometry, namely the construction and calibration of a new system, is not commonplace for a geographer and presented a particular challenge for me. Special thanks are therefore due to Professor Dr. Wolfram Mauser, who made it possible for me to become acquainted with the technology and as the sponsor of this thesis had a significant stake in its progress and success. In many mutual working hours and conversations, he gave me an insight into the fundamental aspects of not only the technical development and execution but also the practical application of AVIS. In the course of this doctoral thesis I constructed my first computer and "got my hands dirty" working on a sensor for the first time; things that I previously would not have considered possible. He also undertook the programming of the flight software as well as the software for the processing of the AVIS data. I would like to thank him cordially for the trust he placed in me, the favourable appraisal of my ideas and the freedom afforded to me in the implementation of the project.

This thesis originated at the Chair of Geography and Geographical Remote Sensing of the Ludwig Maximilians University Munich in connection with a project "Derivation of Plant Chlorophyll and Nitrogen Status with Hyperspectral Remote Sensing Techniques" sponsored by the Deutsche Forschungsgemeinschaft (DFG), who also partly provided financial support for building AVIS. I would like to thank DFG for providing the financial support for this thesis.

The success of this thesis is also closely associated with great teamwork within the Chair of Geography and Geographical Remote Sensing. Special thanks therefore go to all members of this working group, not only for the excellent cooperation and spontaneous support in the solution of problems, but also for the very good and friendly atmosphere. Thanks to Dr. Ingo Keding for his help in technical matters and the seemingly infinite field of statistics. I would like to thank Dr. Roswitha Stolz and Dr. Karl Schneider for letting me profit from their scientific knowledge, especially for questions regarding plant physiology. Cordial thanks to Dr. Heike Bach for her help concerning the radiometric processing of the data. Thanks to Dr. Dieter Rieger for his energetic support in creating the geographic information system of the test areas. I would especially like to thank Dr. Gertrud Strasser in whom I found a friend whose professional and friendly advice I could not have gone without.

I would like to thank Vera Erfurth, Vera Falck and Christian Michelbach for their constant obliging undertaking of design and cartographical tasks.

Not to be forgotten is the support of the many students who assisted in the extensive data collection on site. My thanks go especially to Messrs. Matthias Bernhardt and Tobias Hank,

who assisted me from the beginning of the project and who through their exemplary commitment made a substantial contribution to its success.

Without the obliging help of other institutions, this thesis could not have been completed. I would like to thank Mr. Zimmermann of the Landwirtschaftsamt (Agricultural Science Office) in Starnberg for his helpful information and assistance in the field. The fact that I could refer to previously existing sources made my work much easier.

I would also like to thank Mr. Stuerzer for his obliging help and for providing detailed field data and GPS-based yield measurements for his fields.

This thesis could not have been carried out in this manner without the obliging assistance of the Aviation Sport Group of the airbase at Fürstenfeldbruck (Fürsty). Thanks are therefore due to the Aviation Sport Group for the provision of the plane, often at very short notice. In particular, I would like to thank the pilots Mr. Boehl, Mr. Schifferer, Mr. Trenker and Mr. Herchenröder for their support.

I would like to thank Professor Dr. W. Lutz for making the central laboratory of the Forschungszentrum für Umwelt und Gesundheit (Research Centre for the Environment and Health) GSF available to me for the analysis of the chlorophyll content of the plant samples as well as for technical assistance during the evaluation of the results. My thanks also go to the employees of the central laboratory for their support.

My thanks also go to Professor Dr. J.R. Porra of the University of Melbourne, Australia, who, during his stay in Munich in January 2002, kindly offered to put the chlorophyll analyses performed for the various land-use types to the acid test. In this connection I would also like to thank Professor A. Baker of the University of Essex, UK, who spontaneously and unconventionally assisted me in answering questions on plant physiology.

Thanks are also due to Professor J. Miller of the University of York, Canada, for the fruitful discussions, which provided me with valuable advice regarding the correction and evaluation of spectrometer data.

Naturally, my cordial thanks also go to my family and friends, who stood by me at all times by word and deed. At the same time, I would like to thank Ms. Carmen Scholz and Mr. Markus Schumann for checking through the manuscript. I would especially like to thank my companion Mr. John Asquith for his understanding, his encouragement and his patience during the years full of weekends that "flew by". He gave me the support for these years and had to endure my occasionally shot nerves. Only through his willingness to read the proofs was it possible for me to take the plunge and publish my work in English. I would like to dedicate this thesis to him.

1 Introduction

Man has been monitoring plants for thousands of years, especially since he started to cultivate several species. Ever since these early beginnings, the aim has been to ensure and increase the yield to guarantee the basic food supply. The development of crop rotation in the 1st century A.D. and later on the application of organic fertilisers are examples for the progressive knowledge about plants and their dependence on environmental factors such as soil, temperature, water availability or nutrition. Nowadays, in many countries agriculture is a highly commercialised branch, which is characterised by the calculated use of fertiliser, herbicides, fungicides and machines for attaining the maximum yield.

Remote sensing is increasingly used for crop monitoring and the support of crop management. Satellite based sensors, especially the Landsat series, played and still play an important role in this task. In the last few decades, the impact of vegetation on the water budget or the carbon cycle on regional and global scales has been recognised. Remote sensing data is used to observe changes in vegetation cover and couple the results with models of the water budget and carbon cycle (ESA, 1999).

The development of spectrometers enables not only the investigation of the vegetation cover but also the derivation of individual constituents and furthermore the condition of plants. Ground-based spectrometers are used to derive plant parameters such as leaf area, water content, pigment content and biomass as well as the influence of stress or disease at leaf scale.

With the existence of airborne spectrometers, investigations and existing approaches at leaf scale were continued at canopy level. The first application of an Airborne Imaging Spectrometer (AIS) was described in 1983 (Vane & Goetz). AIS was a proof-of-concept instrument that led to the development of the AVIRIS (Airborne Visible/Infrared Imaging Spectrometer) – the first airborne spectrometer to contiguously cover the solar range from 400 to 2500nm with narrow bands which has been operational since 1989 (Vane & Goetz, 1993). Today, several airborne imaging spectrometers are available such as AVIRIS (Airborne Visible InfraRed Imaging Spectrometer, since 1987), CASI (Compact Airborne Spectrographic Imager, since 1989), ROSIS (Reflective Optics System Imaging Spectrometer, since 1990), DAIS (Digital Airborne Imaging Spectrometer, since 1991) or HYMAP (HYperspectral MAPping, since 1997).

Early research with hyperspectral data was difficult due to the lack of adequate calibration and knowledge of atmospheric effects in order to transform data to surface reflectances as well as the lack of tools to enable the scientists to analyse the data (Vane & Goetz, 1993). These issues have been overcome to a large extent, and several methods are now available for calibration, image processing and analysis of the hyperspectral data.

The first satellite-based imaging spectrometer was launched by NASA in December 2000: HYPERION, an imaging spectrometer with 220 bands in the wavelength region 400-2400nm, a geometric resolution of 30m and a spectral resolution of 5-6nm on board of EO-1 (Earth Observation 1). The first HYPERION data are now available. Examples for European sensors launched or planned are the CHRIS (Compact High Resolution Imaging Spectrometer) on board of Proba or SPECTRA (Surface Processes and Ecosystems Changes Through Response Analysis), both with similar specifications compared to HYPERION.

Airborne data acquisition benefits over satellite-based missions from being operational in the sense that the user can influence the mission in terms of flight line, position, calibration measurements, spectral resolution, ground resolution, acceptable weather conditions and time schedule (Wilson, 1994). Although airborne hyperspectral remote sensing becomes increasingly accessible due to the increasing number of commercial companies operating hyperspectral sensors, the data are often very expensive on account of the limited spatial coverage of an image scene and the fact that multitemporal approaches are often necessary. Furthermore, data processing and georeferencing is complex (Wilson, 1994). Thus the application of airborne imaging spectrometers nowadays is mainly restricted either to investigation on a local scale or to implication studies for forthcoming space-borne hyperspectral data.

At the Institute of Geography and Geographical Remote Sensing of the University of Munich, the above facts combined with the limited availability of airborne imaging spectrometers for multitemporal applications led to the development of an institute-owned system on a low-cost basis, especially for vegetation monitoring applications. The construction of the Airborne Visible / near Infrared imaging Spectrometer (AVIS) was carried out by Prof. W. Mauser with collaboration of Dr. I. Keding in 1998 and laid the foundations for this thesis (Mauser & Oppelt, 2000; Oppelt & Mauser, 2000; Mauser & Oppelt, 2001). The vegetation parameters to be investigated were determined within the scope of the project funded by the German Research Community (DFG) "Derivation of plant chlorophyll and nitrogen status with hyperspectral remote sensing techniques" (DFG MA 875-6). Therefore this thesis focuses on the following areas:

1. Calibration and validation of AVIS,
2. Multitemporal application in the years 1999 and 2000,
3. Processing of the remote sensing data,
4. Derivation of the chlorophyll and nitrogen content of vegetation applying a new approach with existing indices as references,
5. Investigation of the temporal coverage on the one side and the spectral coverage and resolution necessary for this task.

Three different land use types were investigated, namely wheat, maize and grassland, using an empirical approach. As part of this investigation, ground measurements (Ground Truth) were carried out regularly in different test sites in both 1999 and 2000, during which AVIS measurements were also conducted.

The investigation deals with several research questions:

1. Is hyperspectral remote sensing more accurate than multispectral sensors for the derivation of vegetation parameters?
2. What dependency exists between the chlorophyll and nitrogen content of plants using measurements conducted during the ground truth campaigns?
3. What measurements are necessary to derive vegetation parameters chlorophyll and nitrogen on a mean field basis?
4. Can the chlorophyll and nitrogen content of plants be derived applying species optimised as well as species independent vegetation indices?
5. Is it possible to derive the spatial distribution of chlorophyll and nitrogen content within a field?

This results in the following structure of the thesis, which is also presented in Figure 1-1.

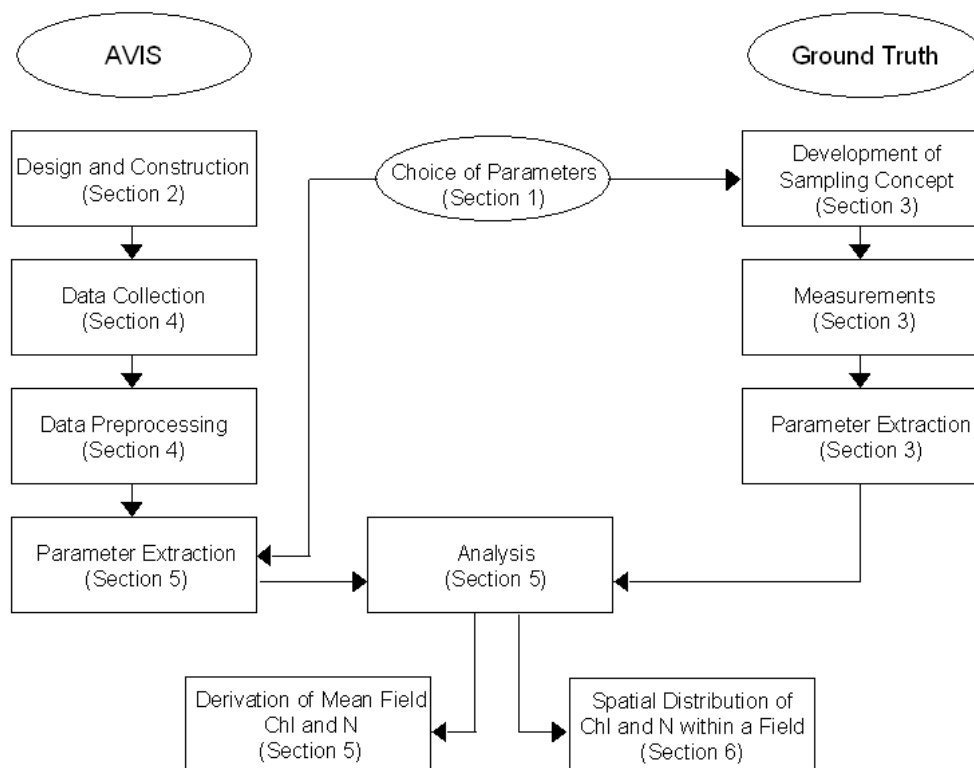


Figure 1-1: Structure of the thesis

An introduction to hyperspectral remote sensing and the importance of the vegetation parameters chosen, namely chlorophyll and nitrogen, follows in section 1. Section 2 describes the most important system parameters of AVIS and the system calibration. Sections 3 and 4 include the ground based and airborne measurements, which were conducted during the vegetation periods 1999 and 2000. In section 3 follows the analysis of the ground truth data, while in section 4 the processing steps for the remote sensing data are described. The measurements of section 3 and 4 form the basics for the analysis of the data regarding the derivation of the chlorophyll and nitrogen content for the investigated land use types, which is focused in section 5. This analysis is based on mean field values derived from either ground or airborne measurements. Finally, the application of the AVIS data for the derivation of the spatial distribution of chlorophyll and nitrogen within a field is described for a field, which is distinguished by an extensive data basis regarding ground based measurements as well as GPS-based yield measurements. This enables a detailed discussion of the derived parameter distribution. The last section includes a summary and an outlook on the further development of the system AVIS as well as the potentialities of the investigated approaches.

1.1 Hyperspectral Remote Sensing and Imaging Spectrometry

Remote sensing is practised by the examination of features as observed in several regions of the electromagnetic spectrum (Figure 1-2).

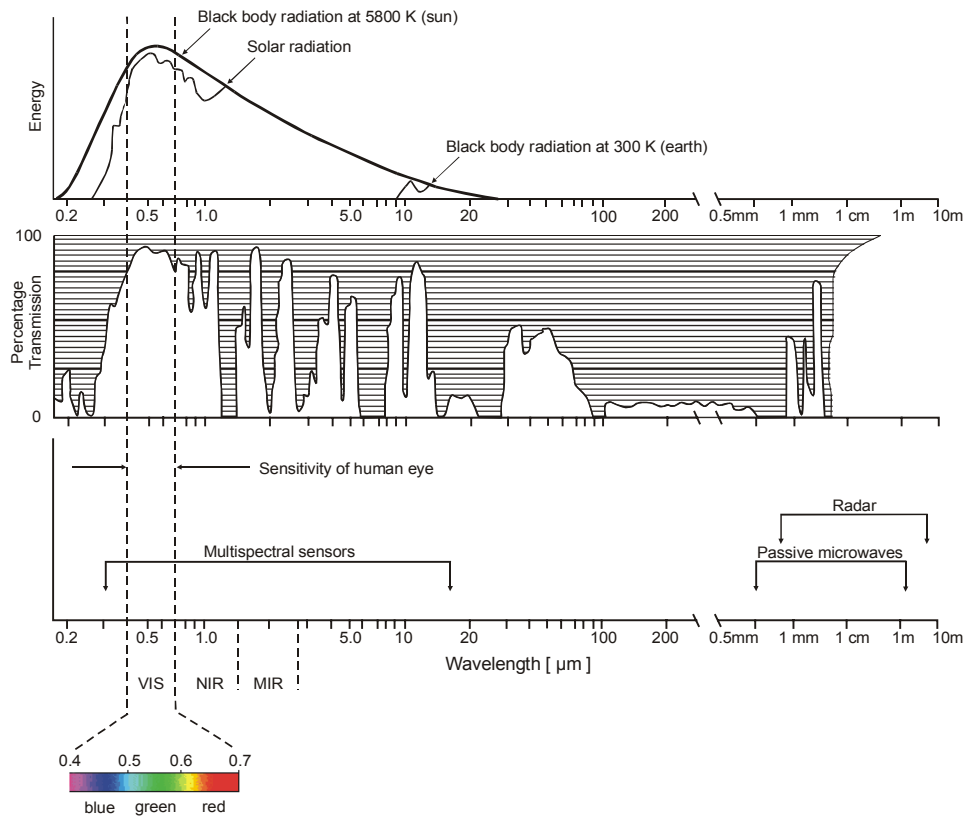


Figure 1-2: Electromagnetic spectrum (Kappas, 1994, modified; cartography: V. Falck)

Conventional remote sensing is based on the use of several rather broadly defined spectral bands, while hyperspectral remote sensing is based on the examination of many narrowly defined spectral bands over a broad range of the electromagnetic spectrum, which enables the recording of a continuous reflectance spectrum. Thus, hyperspectral data have detail and accuracy that permit investigation of phenomena and concepts that greatly extend the scope of traditional remote sensing. Such capabilities present opportunities for much more precise identification of features than is possible with broadband sensors, for use of spectral libraries, for detailed investigation of biologic and geologic phenomena. Due to the measurement that mainly includes the uppermost vegetation or soil layer the obtained spectra are top-of-canopy reflectance spectra (Campbell, 1996; Vane & Goetz, 1993).

Imaging spectrometry is the application of hyperspectral remote sensing for the recording of precise, accurate and detailed spectral measurements of the radiation, which is

reflected or emitted from the earth's surface. This part of the electromagnetic spectrum can be divided into several domains (Campbell, 1996; Wolfe, 1997):

- the visible spectrum (VIS) ranges from 400nm to 700nm and is limited by the sensitivity of the human eye. The visible light can be divided into three primary additives, defined approximately from 400-500nm (blue), 500-600nm (green) and 600-700nm (red), which is also illustrated in Figure 1-2.
- Wavelengths longer than the red portion of the visible spectrum are designated as the infrared region (IR). This segment of the spectrum is large relative to the visible region and extends from 700nm to 15 μ m. The reflected portion of the IR ranges from 700nm to 3 μ m and can be divided into the near infrared (NIR) ranging from 700nm to 1.3 μ m and the mid wave infrared (MIR, 1.3-3 μ m).

Radiation in the NIR and MIR behaves, in respect to the optical systems, in a manner analogous to radiation in the visible spectrum. Whereas near and short wave infrared radiation is essentially solar radiation reflected from the earth's surface, the thermal infrared (TIR) beyond 3 μ m is emitted by the earth.

Hyperspectral sensors necessarily employ designs different from those of usual sensor systems. An objective lens collects radiation reflected or emitted from the earth's surface, a collimating lens projects the radiation as a beam of parallel rays through a diffraction grating or prism, whereby the radiation is dispersed into discrete spectral wavelengths

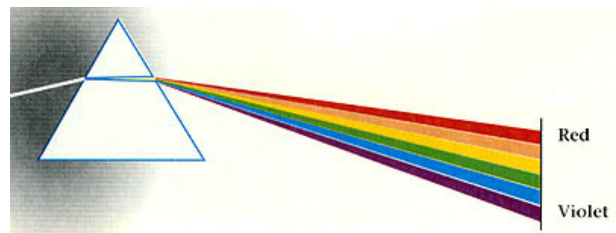


Figure 1-3: Dispersion of light by a prism

(Figure 1-3). The energy in each spectral band is then detected by one or several arrays as image line. The superimposition of the same surface, observed at different wavelengths lead to an image cube (Figure 1-4). The two dimensions formed by the x and y axes of the usual map or image display is formed by the movement of the sensor over the ground, while the third (z) is formed by the accumulation of spectral data as bands. The top of the cube is an image composed of data collected at the shortest wavelength, and the spectral band of the longest wavelength of the sensor forms the bottom. Intermediate wavelengths are found as slices through the cube at intermediate positions. Values for an individual pixel observed along the edge of the cube form a spectral trace describing the spectra of the surface presented by the pixel (Campbell, 1996; Wolfe, 1997).

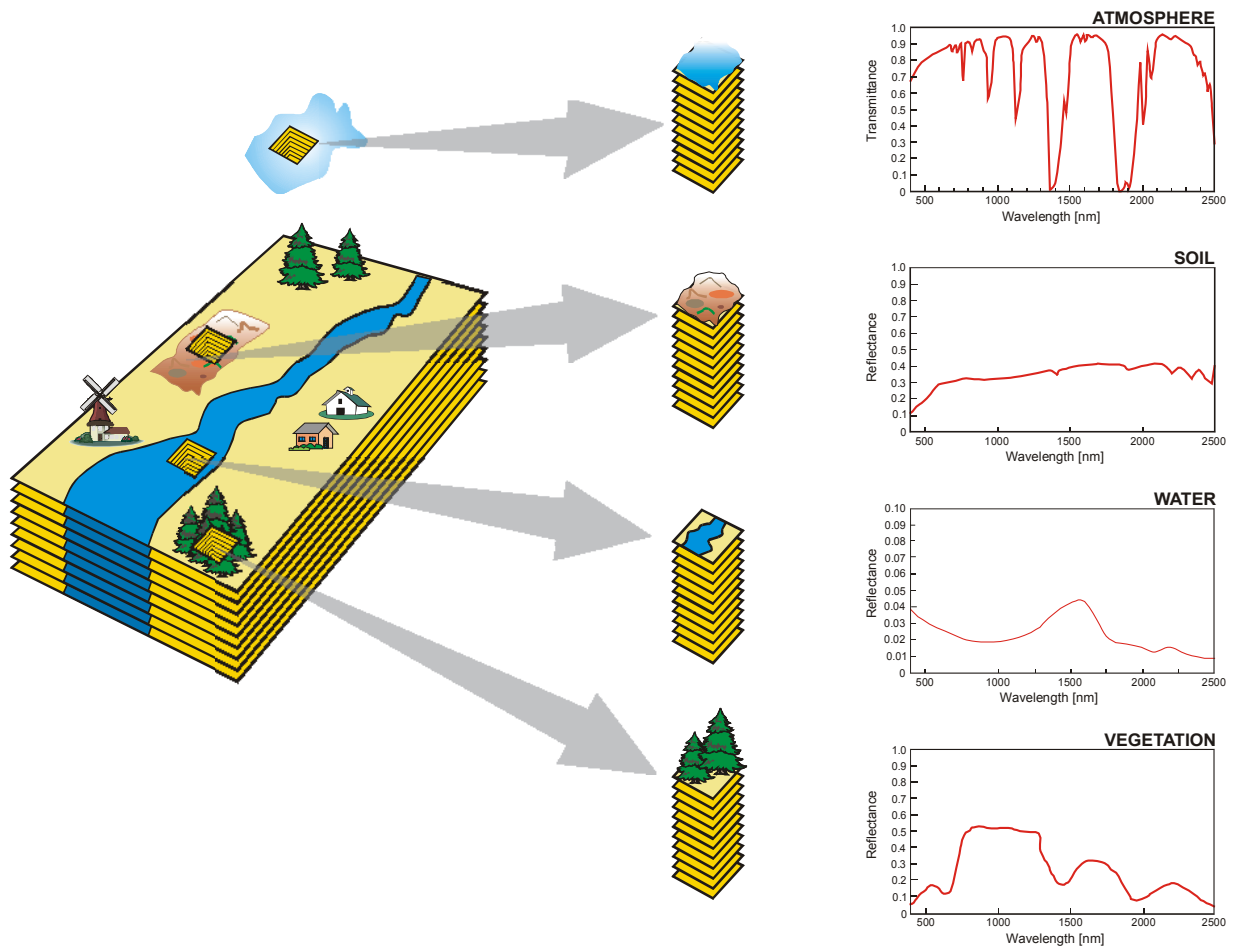
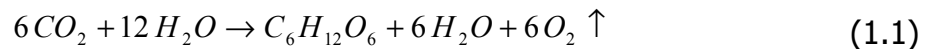


Figure 1-4: Hyperspectral image cube (based on NASA diagram; cartography: V.Falck)

1.2 Importance of Chlorophyll and Nitrogen

Chlorophyll is the pigment primarily responsible for harvesting light energy used in photosynthesis. Photosynthesis is unique in utilising light as a source of energy for the incorporation of carbon dioxide and water into an energy-rich product, sugar that can be metabolised by the plants (equation (1.1)) (Kaufman et al., 1989):



The common denominator in all photosynthetic plants is the occurrence of chlorophyll a. Special molecules of chlorophyll a are believed to accept light energy (electrons) from surrounding pigments and transfer it to an acceptor molecule, resulting in the conversion of light energy to a stable form of chemical energy, which is stored in the form of assimilated carbon. For this, chlorophyll a is viewed as playing the key role in the transfer of light energy. The other pigments are referred to as accessory pigments and include chlorophylls b, c and d, carotenoids, photocyannin and photoerythrin (Kaufman et al., 1989). The specific structure as well as the absorption features of the chlorophylls are described in more detail in section 5.1.

The primary event in photosynthesis is the absorption of light by the photosynthetic pigments, i.e. the chlorophylls, which are located in the chloroplasts. Chlorophyll primarily is located in the leaves. Mainly this proportion is also viewed by a remote sensing system due to the more or less horizontal alignment of the leaves. The chlorophyll content is correlated with the depth and width of its absorption feature and can be measured by hyperspectral remote sensors.

As mentioned above, photosynthesis forms the basis of plant growth, development and primary productivity. A clear and detailed knowledge of bio-chemical processes as well as their change due to climatic and anthropogenic pressure is essential for the understanding of the environment. Therefore chlorophyll is an important parameter for an accurate characterisation of these processes as well as for their inclusion into hydrological or vegetation modelling.

There are four atoms of nitrogen in each molecule of chlorophyll. This close relation together with the fact that nitrogen itself does not absorb or reflect radiation leads to the derivation of nitrogen content via the chlorophyll content of the plant or leaf respectively.

Most plant tissues contain between 1 and 5% nitrogen on a dry weight basis, and its content tends to decline during the maturation. About 80% of the initial leaf nitrogen content is recycled before leaf abscission. The fraction in dead leaves presumably corresponds to structural leaf nitrogen, whereas the fraction remobilised corresponds to the metabolic pool. For the optimisation of canopy photosynthesis, the metabolic nitrogen pool can be remobilised to vivid parts of the plants (Lemaire, 1997).

Nitrogen is very important in plant nutrition. It is a component of all amino acids and proteins, including the enzymes vital to plant metabolism. It is a constituent of the building blocks of nucleic acids and is found in vitamins and many other plant constituents. Nitrogen is required in relatively large amounts for optimum growth and it is the availability of nitrogen that often causes the limitation to growth. To be available for the plants, it must be fixed, meaning that it must be combined with some other element to form a nitrogen compound. Examples for compounds are nitrate (NO_3^-) or ammonium (NH_4^+), which are available to plants (Kaufman et al., 1989) and are absorbed through the roots. In addition to that, plants can absorb some forms of nitrogen (particularly gaseous ammonia and nitrogen dioxide) through their leaves, but absorption through the leaves contributes only a small proportion (<5%) of the total uptake (Whitehead, 1995).

The knowledge of the impact of nitrogen to the plant as well as the low prices for nitrogen fertiliser led to increasing fertilisation with nitrogen during a period from about 1950 to the mid 1980s (Whitehead, 1995). Although other factors were involved, the increasing rate of nitrogen fertiliser was responsible for much of the amounts of nitrogen leached through the soil and lost in gaseous forms to the atmosphere. Nitrogen that is leached from soils into groundwater is almost entirely in the form of nitrate and, if the groundwater is used for domestic supplies, the nitrate may constitute a health risk to consumers. In 1980 the European Community adopted a directive, which includes a maximum concentration of nitrate in water intended for human use. This directive as well as the perception of the negative impact of overfertilisation to the yield led to a more sensitive handling of nitrogen fertilisation. Therefore the nitrogen content of plants is an important parameter for the nutrition management by farmers to optimise the plant development and thus yield.

In recent years, the spatial distribution of the nitrogen within the fields becomes increasingly important in the scope of optimising the field management. GPS-based yield measurements showed the heterogeneity of the yield within a field and therefore non-uniform plant nutrition status and enabled the spatially distributed employment of fertiliser. The advantage of hyperspectral remote sensors for this task is obvious as soon as they have shown their ability to derive plant constituents and the generation of two-dimensional data.

2 AVIS – the Airborne Visible/Near Infrared Imaging Spectrometer

The costs for the use of existing imaging spectrometers such as DAIS, AVIRIS or HYMAP are high. Also, it is difficult to obtain these sensors for multitemporal applications such as monitoring of vegetation. Therefore, there is a need for a cost effective as well as available tool in hyperspectral remote sensing.

To fill this gap, the imaging spectrometer AVIS (**A**irborne **V**isible / near **I**nfrared imaging **S**pectrometer) was built at the Chair of Geography and Geographical Remote Sensing of the Ludwig Maximilians University Munich, Germany.

The characteristics of AVIS, which include radiometric, spectral and spatial properties, depend strongly on the characteristics of its individual components. The quality of each property, which determines the performance of the AVIS system, is limited by the quality of the parameters of the individual components. Therefore, the most important characteristics of the AVIS components, related to the subject of this study, will be described as well as the resulting overall performance of the system. The calibration procedure as an important part for the assessment of the capabilities of the system will also be described.

2.1 System Description

The system was developed using commonly available components, leading to the Airborne Visible/near Infrared imaging Spectrometer AVIS (Figure 2-1 and Figure 2-2). AVIS is a line imaging spectrometer consisting of two main parts: the camera unit, which includes the camera, spectrometer, lens and filter, and the storage unit, which includes the PC, frame grabber and dGPS.

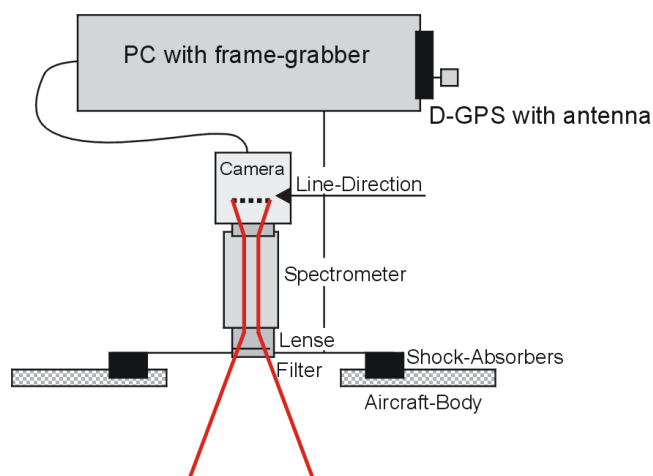


Figure 2-1: AVIS schematic (Oppelt & Mauser, 2000)

The power supply of AVIS is ensured by two 12V lead batteries, which provide power for a runtime for at least three hours.

Figure 2-2: AVIS mounted into the aircraft

2.1.1 Camera Unit

The main part of the camera unit is the spectrograph, which is directly coupled to a standard B/W CCD camera via a C-mount. A lens is mounted in front of the spectrograph, and finally a filter is mounted in front of the lens (see also Figure 2-3).

The incoming light passes the filter and is focussed by the lens. Then it passes the spectrograph and is dispersed into the different wavelengths along its spectral axis. Finally, it is registered on the CCD element of the camera as an electrical charge, which is then read out and sent to the storage unit in form of a voltage signal.



Figure 2-3: AVIS camera unit with CCD camera, spectrograph, lens and filter (SPECTRAL IMAGING LTD., 1998a)